A Pulsed Time-of-flight Mass Spectrometer for Liquid Secondary Ion Mass Spectrometry

J. K. Olthoff[†], I. A. Lys and R. J. Cotter[‡]
Department of Pharmacology and Molecular Sciences, Johns Hopkins University, Baltimore, MD 21205, USA

The design and performance of a new time-of-flight mass spectrometer is reported. The instrument combines the advantages of a pulsed drawout TOF analyzer with a liquid secondary ion source. Differences from commercially available pulsed TOF analyzers (Wiley/McLaren type) are discussed with regard to operation with ion desorption from a liquid matrix.

In 1955, Wiley and McLaren[1] published a time-of-flight (TOF) technique which became the standard for many of the commercially available TOF mass spectrometers in use today. Their design provided simultaneous "space focusing" (compensation for initial spatial ion spread) and "energy focusing" (compensation for initial energy spread) for improved mass resolution. Space focusing was achieved using a two-stage ion extraction system, while energy focusing was obtained by using a delay time between the ionization and extraction pulses and was known as time-lag focusing. The commercially available version of this instrument (from Bendix, and then from CVC) became an instrument regularly used for gas analysis and GC/MS detection.

In recent years, fast analog data acquisition systems have been developed which allow detection of ions of all masses produced by a single ionization event in a TOF mass spectrometer. Coupled with short, pulsed ionization techniques (particularly lasers), this has greatly increased the importance of Wiley/McLaren TOF mass spectrometers. Wiley/McLaren instruments are currently attached to multiphoton ionization sources,[2,3] molecular beam sources[4] and laser desorption sources.[5,6]

Recently we have developed an approach which interfaces a pulsed high-flux liquid secondary ion mass spectrometer (SIMS) source to a Wiley/McLaren type mass analyzer. The instrument is intended to take advantage of the high mass, high sensitivity characteristics of the TOF analyzer in conjunction with the benefits of a liquid matrix generally employed in the fast atom bombardment technique. A pulsed TOF mass spectrometer is ideally suited for this application since its low-voltage, field-free source does not interact adversely with a liquid sample. The capability of varying the time period between ionization and extraction provides an opportunity of studying decomposition of metastable gas phase ions desorbed from the sample.[7] Also, the ability to use high density primary ion pulses has provided the opportunity of varying the ionization pulse frequency and promoting insight into the repair mechanisms of liquid matrices.[8]

Initial studies of the high flux liquid SIMS-TOF mass spectrometer were done by attaching a pulsed ion gun to a commercial Wiley/McLaren type TOF mass spectrometer.[9] A new instrument has since been designed and constructed which follows the basic characteristics of Wiley and McLaren's pulsed TOF design, but with improvements which make the instrument more appropriate for desorption of ions from a liquid source by a pulsed ion beam. This instrument is described in detail in this paper.

INSTRUMENT DESCRIPTION

The instrument consists primarily of a pulsed ion gun attached to a pulsed time-of-flight mass spectrometer (Fig. 1). $Xe^{+\cdot}$ ion pulses are created in the ion gun and strike a liquid sample located on a copper probe. Secondary ions are desorbed from the liquid sample and remain in the field-free source during a delay time of 0 to 50 μs. This delay is used either for energy focusing (as in Wiley/McLaren TOF mass spectrometers) or to observe decomposition of metastable sample ions. After the time delay, secondary ions are extracted into the analyzer by symmetric pulses applied to the drawout grid and backing plate. The ions are then further accelerated into the drift tube by a −200 V acceleration pulse, an intermediate grid at approximately −1500 V, and the front of the flight tube at −3 kV. Two sets of orthogonal deflection plates in the flight tube focus the ions onto the detector for greater sensitivity. A third set of deflection plates deflects low mass ions away from the exit aperture of the drift tube to prevent detector saturation. Secondary ion currents are amplified by a dual channel plate detector with

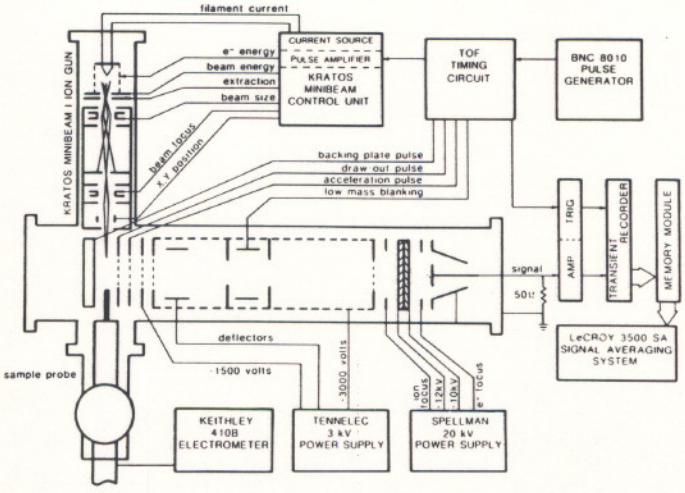

Figure 1. Diagram of high-flux liquid SIMS-TOF apparatus configured for positive ion detection.

[†] Present address: National Bureau of Standards, Room B-344, Bldg. 220, Gaithersburg, MD 20899, USA.
[‡] Author to whom correspondence should be addressed.

CCC-0951-4198/88/0171-0175 $2.50

post-acceleration, and are digitized by a LeCroy 3500 SA signal-averaging system.

The vacuum system consists of a single Balzers 270 turbomolecular pump located directly beneath the source. The large pumping speed of the turbo pump (270 L/s) and the simplicity of the vacuum system permit pressures of 1×10^{-6} Torr to be maintained with the xenon ion gun operating and a liquid sample in place. All electronics are wired through a fail-safe circuit triggered by a CVC GIC-400 ion/thermocouple gauge against large accidental pressure increases.

The remainder of this section of the paper will discuss in greater detail the instrument's timing circuitry, ion gun, pulsing electronics, detector, low-mass blanking, and negative ion capabilities.

A. Time-of-flight timing circuitry

The timing sequence of the mass spectrometer is illustrated in detail in Fig. 2. A variable trigger (from 10 Hz to 10 kHz) from a BNC 8010 pulse generator initiates the sequence by triggering the timing circuit. The timing circuit then pulses the ion gun which generates a primary ion pulse of variable width. After a delay time of 0 to 50 µs, the ions are accelerated into a flight tube by extraction pulses applied to the backing plate, draw-out grid and acceleration grid (see pulse electronics section). A timing trigger which is coincident with the beginning of the extraction pulses initiates the timing by the LeCroy data system. Pulses are applied to the low-mass blanking plates from the first trigger up until some time following the extraction pulses (see low-mass blanking section). The TOF timing circuit which generates all of the appropriate signals for this timing sequence is illustrated in Fig. 3 and is described in detail below.

The TOF timing circuitry is housed in a NIM module, and contains only the delay electronics. All of the delay circuitry is digital, and operates from a common 10 MHz clock (U4). The incoming pulse from the 8010 is buffered and sent directly to the Minibeam ion gun. The 8010's analog circuitry controls the width of this pulse. The first set of three counters (U1-U3) allows the mass analyzer pulse circuitry to operate at a much lower rate than the gun. This feature has been

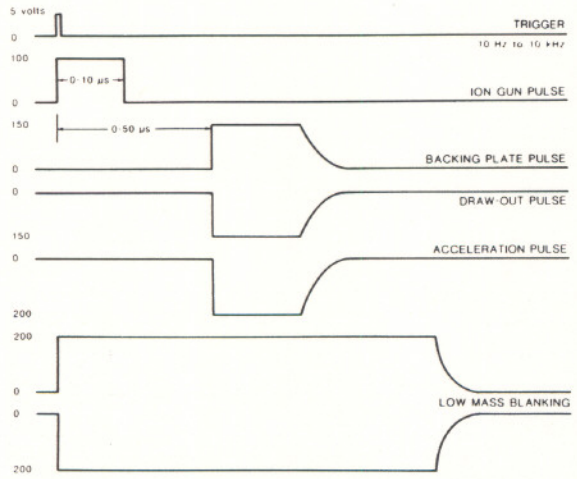

Figure 2. Timing diagram for liquid SIMS pulsed TOF mass spectrometer configured for positive ion detection.

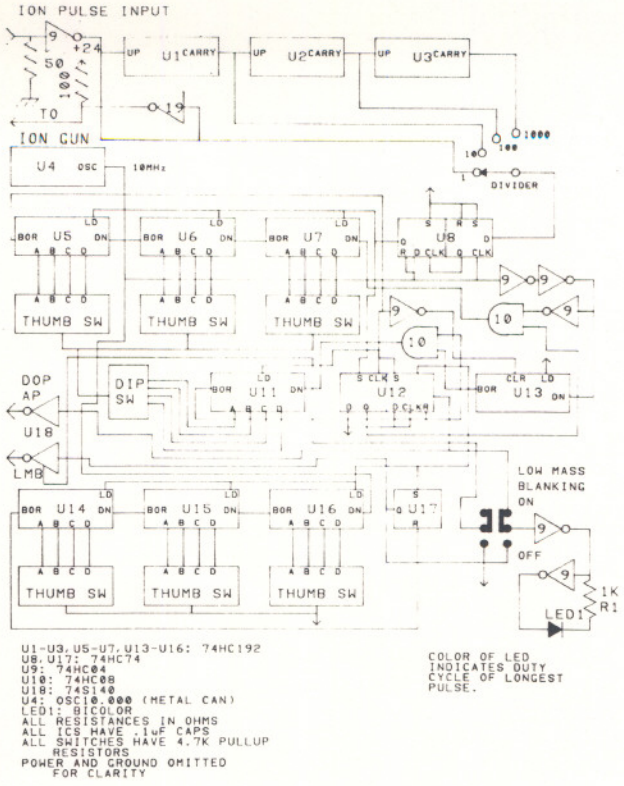

Figure 3. Schematic diagram of main timing circuit.

employed in previous studies on the effects of ion pulse repetition rates on secondary ion yield, where it was desirable to maintain a constant repetition rate for the analyzer.[8] U1, U2, and U3 count each incoming pulse, and each sends out one pulse for every 10 received, allowing division by 1, 10, 100, and 1000. U8 synchronizes the pulse with the 10 MHz clock, and finds the falling edge of this pulse. It makes a 100 ns negative-going pulse, which loads the time-delay counters (U5-U7) and triggers the low-mass blanking flip-flop to start the pulse. U5, U6 and U7 are loaded with the setting of the panel switches by the synchronized pulse from U8. U12, which is also set by the pulse from U8, turns on the clocking signal to these three counters, and eventually is reset at the conclusion of the time lag by the borrow pulse from the counters. This borrow pulse from U5 also sets U11, resets U13, and sets the second half of U12. Since the low logic level on the borrow line disappears as U11 is loaded, the 1 MHz pulse train from U13 decrements U11 until the zero count is once again reached, whereupon counting is once again inhibited. The output of U12 is buffered by U18, and becomes the drawout pulse. It also loads the low-mass-blanking delay counters with the panel switch values and enables counting. The 10 MHz clock decrements the counters, and upon reaching a count of zero, the borrow pulse resets U17 and ends the low-mass-blanking pulse. U18 buffers this pulse, and allows it to be disabled if low-mass blanking is not desired. The light-emitting diode gives a visual indication of the duty cycle of the longest pulse, and slowly turns red as the duty cycle increases, providing an indication of when the pulse shape begins to deteriorate due to excessive duty cycles.

B. Ion gun

The ion gun used in the instrument is a modified Kratos Minibeam I ion gun. $Xe^{+\cdot}$ ions are created by electron impact in the ion-gun source and are accelerated and focused by succeeding elements. Continuous primary ion current densities ranging from 0.1 $\mu A/cm^2$ to 100 $\mu A/cm^2$ are obtainable. Ion-beam spot diameters may be varied from approximately 200 μm to 2 mm, and the beam may be positioned and rastered over any portion of the sample.

For this instrument, the ion gun electronics have been modified to allow the gun to produce ion pulses in addition to a continuous beam. This is accomplished by applying a 120 V pulse to the electron acceleration grid in the ion-gun source. During a pulse, the electrons are accelerated and ionization occurs, thus creating a packet of $Xe^{+\cdot}$ ions whose width is determined by the length of the trigger pulse. Ion pulses of 0 to 10 μs in length with rise and fall times of less than 1 μs are used.

The fact that all characteristics of the primary bombarding beam (current densities, spot size, pulse width, pulse frequency) are measurable and variable makes this ion gun well suited for desorption mechanism investigations. For example, studies have shown that variations of primary ion current densities affect the amount of fragmentation[10] observed in spectra. It has also been noted that changes in primary-ion pulse frequency affect secondary ion yield.[8] These types of experiments can only be carried out with a pulsed high-flux ion source. The modifications which were made to the Minibeam gun electronics are illustrated in Fig. 4 and described below.

The Minibeam gun requires a filament-current control, and a pulsed grid control. This circuitry must float with the high-voltage supply, and must therefore be completely isolated from ground. The filament-current control circuit consists of Q1, Q2, and Q3. Q1 and Q2 buffer the voltage at the slider of R2, the current control. This voltage is then applied to the base of Q3, which compares this voltage with that at its emitter, and is forced to conduct a current when this voltage exceeds 0.7 V. This current then flows through the filament and R5, heating the filament, and indicating the current through the meter. A voltage is developed across R3 and R4, which varies the filament current, and provides feedback to Q3. This voltage rises as the current rises, eventually bringing Q3 to a stable conduction current. The pulse circuitry has a

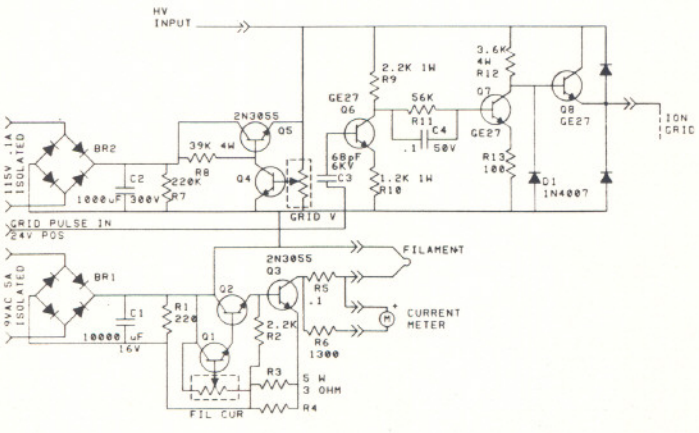

Figure 4. Schematic diagram of modifications made to electronics of Kratos Minibeam I ion gun to achieve pulsed operation.

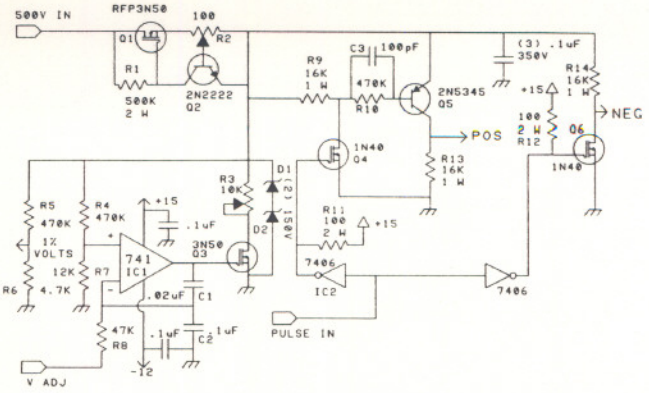

Figure 5. Schematic diagram of pulse circuitry used for drawout pulses, acceleration pulses, and low-mass blanking pulses.

power supply, which is adjustable from 0 to 150 V. This circuit is a feedback type regulator, consisting of Q4 and Q5. R14's slider controls the voltage at the base of Q4. When this voltage exceeds 0.7 V, Q4 is forced to conduct, reducing the voltage at its collector, and thereby reducing the drive to Q5, lowering the voltage at the output. The transfer characteristics of this circuit are logarithmic, compensating for the antilogarithmic behaviour of the ion gun. The pulse circuit consists of Q6, Q7 and Q8. The 15–24 V positive input pulse is isolated from the high voltage by C3, and inverted by Q6. R11 and C4 form a coupling circuit which drives Q7. Q7, normally saturated, is brought out of conduction by the negative-going pulse at its base, and allows R12 to force Q8 into saturation, discharging any stray capacitance and creating a large positive pulse at the output. D1, D2, and D3 are protective diodes, which attempt to limit any spikes caused by occasional discharges inside the ion gun.

C. Extraction pulses

After secondary ions are desorbed by the primary ion pulse, they are accelerated into the drift tube by symmetric extraction pulses applied to the backing plate and the drawout grid. These pulses are symmetric about ground potential to maintain uniform acceleration fields in the source even with a grounded copper probe protruding into the centre of the source region. The amplitude of the pulses is approximately ±150 V with rise times of less than 20 ns. Space focusing is achieved by varying the amplitude of these pulses for best resolution. Similar but larger pulses are applied to the acceleration grid following the drawout grid.

All of these pulses (including those used for low-mass blanking to be discussed in a later section) are produced with identical circuitry (see Fig. 5). Three identical boards, each containing this circuit, are located directly on the source flange to provide pulses for extraction, acceleration and low-mass blanking. Voltage references and triggers are all provided by the TOF timing circuit.

The operation of the pulse circuits is as follows. Each board contains three major sections. The first is a constant current regulator, adjustable from 7 to 40 mA. This circuit is composed of Q1, Q2, R1, and R2. The current flowing through R2 creates a voltage across the B-E junction of Q2, which begins to turn on, causing a voltage drop across R1, and reducing the gate drive on

the MOSFET Q1. Q1 supplies the actual operating current for the rest of the pulse circuitry. Since Q2 is a silicon transistor, the B-E turn-on voltage is about 0.5 to 0.7 V, which is dropped across potentiometer R2.

The voltage regulation circuitry is composed of R3-R8, C1, C2, D1, D2, IC1, and Q3. Diodes D1 and D2 limit the B+ to protect the transistors, and clamp any negative transients or negative voltages. R3 provides a low voltage limit, to protect Q1 from excessive power dissipation, and stabilizes the supply by increasing the impedance of the shunt regulator. Resistors R4 and R7 provide feedback for the regulator, and, along with R5 and R6, provide a resistive load. This also prevents a no-load condition from occurring, and prevents semiconductor leakage current from affecting the circuit. Together, these resistor networks draw about 1 mA at 250 V. Resistors R4 and R7 provide an internal indication of the voltage to IC1, a comparator. Capacitors C1 and C2 along with R8 form a negative AC feedback path to IC1 to prevent oscillation, and enhance stability. Q3 is driven by IC1, and performs the actual regulation of the output voltage. Resistors R5 and R6 provide test voltages which are at 1% of the actual pulse voltage.

The pulse section is composed of Q4-Q6, R9-R14, C3, and IC2. Q4 and Q6 have essentially the same function. A negative-going pulse appears at the PULSE IN pin, and is terminated by a 120 ohm resistor R_{term} to ground. The signal is inverted by a 7406 (actually three inverters are in parallel). R11 (or R12) pulls up the gate voltage on the MOSFET (Q4 or Q6) and causes rapid build-up of the charge on the gate, driving the MOSFET into saturation. This causes a negative pulse either at the negative output (as in the case of Q6) or at R10 and C3 (for Q4). The high current negative pulse from Q4 is applied to the base of inverting transistor Q5, through C3 and R10. This quickly drives Q5 into saturation and causes a positive pulse to appear at the positive output. C3 builds up the initial charge on the base of Q5, and causes the fast leading edge of the pulse, while R10 provides the later base drive for the remainder of the pulse. As the input pulse ends, charge depletion occurs at the gate of Q4 and Q6, which slowly come out of conduction and their associated pull-up resistors recharge the highly capacitive outputs of the MOSFETs. The base drive to Q5 is quickly depleted by the rising pulse at Q4, and Q5 follows Q4's slow trailing edge.

D. Post-acceleration detector

The detector used in the istrument is a dual channel plate detector floating at a high potential (−12 kV) to provide post-acceleration of the ions. The detector assembly, purchased from Galileo, has been modified by moving the channel plates away from the grounded collector anode, and by adding focusing plates before and after the channel plates. The front end of the first channel plate is held at −12 kV (for positive ion detection), thus accelerating ions to a higher velocity before striking the channel plates and greatly increasing high-mass detection sensitivity. Voltages on the ion-focus plate and the electron-focus element are adjusted for maximum sensitivity. All voltages are derived from a ±20 kV Spellman power supply and a voltage divider. Secondary electrons are collected by the collection anode and the signal is digitized by the data system.

E. Low-mass blanking

One of the disadvantages of using channel plates for analog detection is the long recovery time of the individual channels (>10 ms).[11] A channel plate contains approximately 10^5 channels in the active region of the detector. An estimate of the number of secondary ions produced by a single primary ion pulse in the source of this instrument is approximately 10^5 to 10^6. Thus, the first ions from a single ion packet can saturate the detector (i.e., deactivate a large percentage of the channels) before the last ions arrive. This lowers the sensitivity for high-mass ion detection since they arrive last at the detector. The situation is aggravated by the fact that a large majority of the ions created in the source (approximately 90 %) are very low mass ions (often related to the matrix) which contain little or no information. Thus low-mass deflector plates have been installed part way down the drift tube to deflect low mass ions away from the exit aperture. ±250 V pulses are applied to these plates during times when the low mass ions are passing and the plates are returned to the flight tube voltage when higher mass ions of interest go by. By varying the length of the low-mass blanking pulses, the minimum-mass detection cut-off may be varied to any desired value.

F. Negative ion analysis

The analysis of negative ions may be done with only a few changes. The polarities of all high voltage power supplies must be switched. Next, the extraction pulses must be made the opposite polarity by simply switching the cables from the pulse boards. Lastly, the detector voltages must be reconfigured. For example, the ion focus, front channel plate, back channel plate, electron focus, and anode may be set at +4 kV, +6 kV, +8 kV, +10 kV and +10 kV, respectively. However, since the anode is now at high potential, the signal must be sent through a high voltage capacitor to the data system.

RESULTS AND DISCUSSION

Cluster ions of cesium iodide, having the formula $[CsI]_nCs^+$, are generally used to calibrate fast atom bombardment mass spectra on sector instruments, since such ions can be generated over a wide mass range. The mass spectrum of cesium iodide, obtained on the liquid SIMS time-of-flight mass spectrometer, is shown in Fig. 6. Positive cluster ions are observed beyond 12 000 mass units.

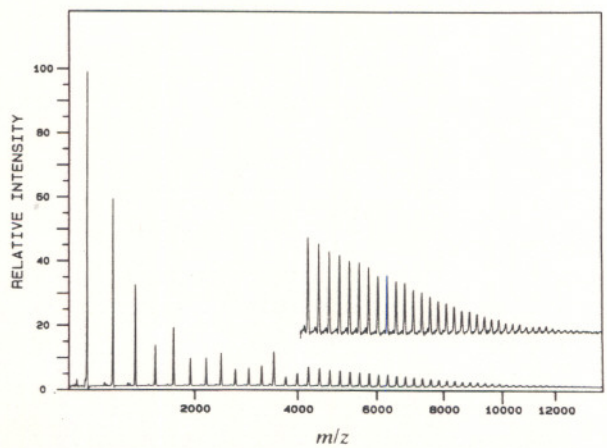

Figure 6. Liquid SIMS-TOF mass spectrum of cesium iodide.

Figures 7 and 8 show the positive and negative ion mass spectra, respectively, for the peptide Gramacidin S. Protonated molecular ions, MH^+, are formed in the positive mode, while $[M-H]^-$ ions are formed in the negative ion mode. In addition, some sequence ions are also observed. Figures 9 and 10 give some additional examples of positive ion mass spectra for the peptides Substance P and Bacitracin, respectively.

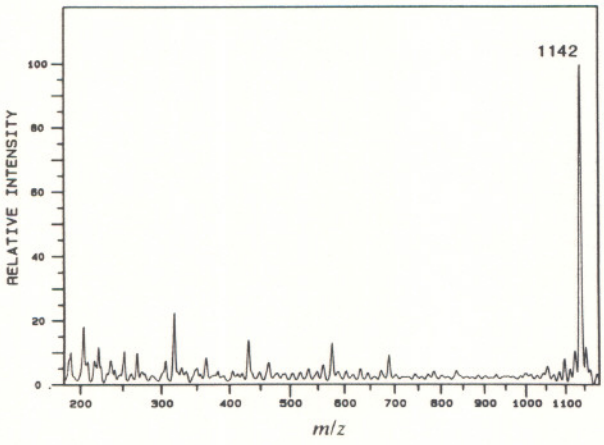

Figure 7. Positive ion liquid SIMS-TOF mass spectra of Gramicidin S.

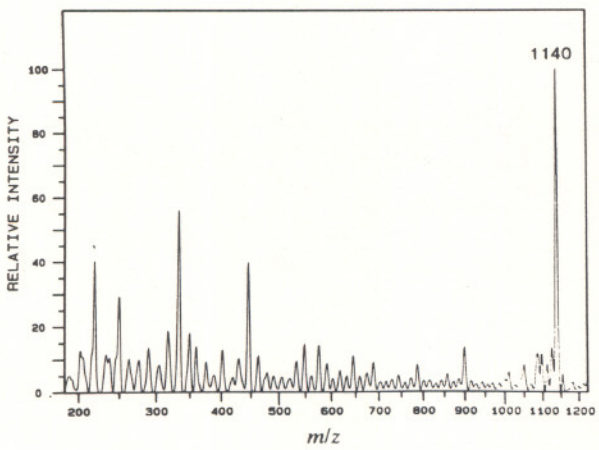

Figure 8. Negative ion liquid SIMS-TOF mass spectra of Gramicidin S.

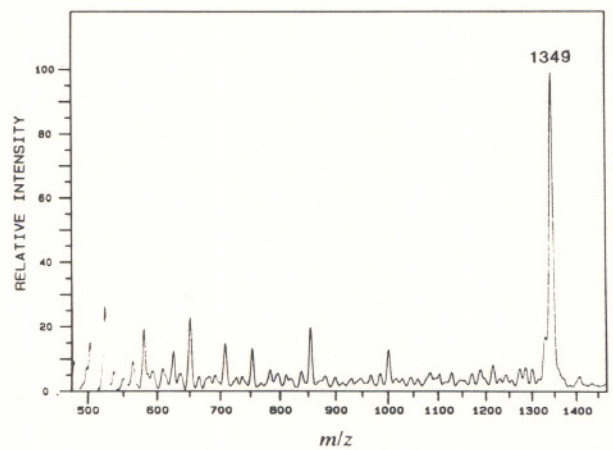

Figure 9. Liquid SIMS/TOF mass spectra of Substance P. (Arg-Pro-Lys-Pro-Gln-Gln-Phe-Gly-Leu-Met).

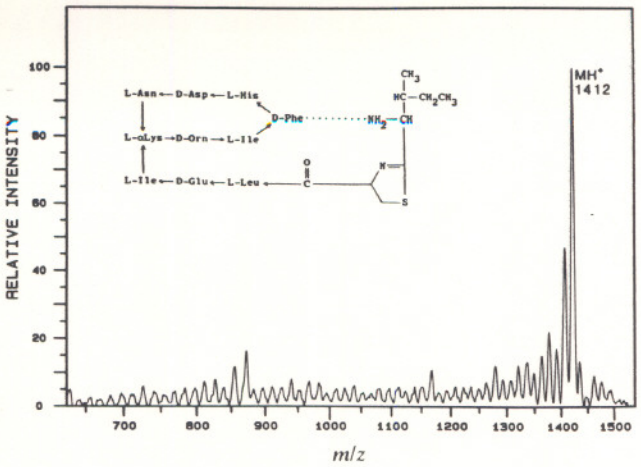

Figure 10. Liquid SIMS-TOF mass spectra of Bacitracin.

With the exception of the cesium iodide, all of the spectra were obtained from samples dissolved in glycerol on thioglycerol and deposited on the probe tip. Because of the low-duty-cycle sputtering using the pulsed gun, the sample lifetimes are considerably longer than for scanning instruments and spectra may be obtained for several minutes. The cesium iodide spectra are stable for up to 30 min and can be observed on an oscilloscope for dynamic timing of the drawout, acceleration and deflector voltages and the time lag for optimal focusing.

Because the instrument is compatible with a liquid matrix, the potential exists for interfacing the liquid SIMS-TOF with a high performance liquid chromatograph, using a continuous flow probe.[12] Preliminary experiments with such a system are currently underway.

Acknowledgement

This work was funded by a grant (GM 33967) from the National Institutes of Health and carried out at the Middle Atlantic Mass Spectrometry Facility, an NSF Shared Instrumentation Facility.

REFERENCES

1. W. C. Wiley and J. H. McLaren, *Rev. Sci. Instr.* **26**, 1150 (1955).
2. W. B. Martin and R. M. O'Malley, *Int. J. Mass Spectrom. Ion. Proc.* **59**, 277 (1984).
3. G. R. Kinsel, K. R. Segar and M. V. Johnston, *Proc. 35th Annual Conf. on Mass Spectrom. Allied Topics,* Denver p.405 (1987).
4. J. E. Pollard and R. B. Cohen, *Rev. Sci. Instr.* **58**, 32 (1987).
5. R. B. VanBreemen, M. Snow and R. J. Cotter, *Int. J. Mass Spectrom. Ion Phys.* **49**, 35 (1983).
6. J. K. Olthoff, I. Lys, P. Demirev and R. J. Cotter, *Anal. Instr.* **16**, 93 (1987).
7. P. Demirev, J. K. Olthoff, C. Fenselau and R. J. Cotter, *Anal. Chem.* **59**, 1951 (1987).
8. J. K. Olthoff and R. J. Cotter, *Nucl. Instr. Meth.* **26**, 566 (1987).
9. J. K. Olthoff, J. P. Honovich and R. J. Cotter, *Anal. Chem.* **59**, 999 (1987).
10. J. K. Olthoff, I. Lys and R. J. Cotter, *Proc. 35th Annual Conf. on Mass Spectrom. Allied Topics*, Denver, p. 735 (1987).
11. J. L. Wiza, *Nucl. Instr. Meth.* **162**, 587 (1979).
12. K.-H. Chen, P. Marcus and R. J. Cotter, presented at *36th Annual Conf. on Mass Spectrom. Allied Topics*, San Francisco (1988).

Received 29 June 1988; accepted 12 July 1988.